JCTC Journal of Chemical Theory and Computation

Open Access
This article is licensed under CC-BY 4.0

pubs.acs.org/JCTC Article

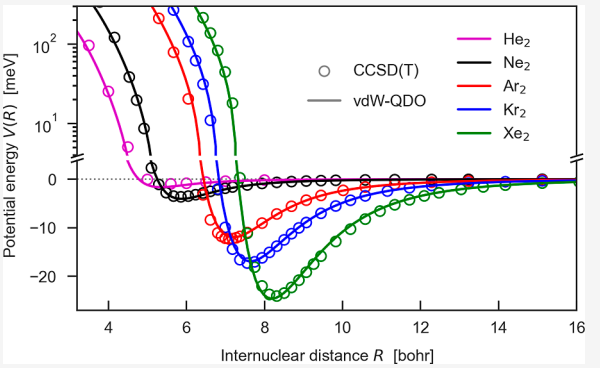
Universal Pairwise Interatomic van der Waals Potentials Based on Quantum Drude Oscillators

Almaz Khabibrakhmanov, Dmitry V. Fedorov, and Alexandre Tkatchenko*

Cite This: J. Chem. Theory Comput. 2023, 19, 7895−7907 Read Online

ACCESS | Metrics & More | Article Recommendations | Supporting Information

ABSTRACT: Repulsive short-range and attractive long-range van der Waals (vdW) forces play an appreciable role in the behavior of extended molecular systems. When using empirical force fields, the most popular computational methods applied to such systems, vdW forces are typically described by Lennard-Jones-like potentials, which unfortunately have a limited predictive power. Here, we present a universal parameterization of a quantum-mechanical vdW potential, which requires only two free-atom properties—the static dipole polarizability α_1 and the dipole−dipole C_6 dispersion coefficient. This is achieved by deriving the functional form of the potential from the quantum Drude oscillator (QDO) model, employing scaling laws for the equilibrium distance and the binding energy, and applying the microscopic law of corresponding states. The vdW−QDO potential is shown to be accurate for vdW binding energy curves, as demonstrated by comparing to the ab initio binding curves of 21 noble-gas dimers. The functional form of the vdW−QDO potential has the correct asymptotic behavior at both zero and infinite distances. In addition, it is shown that the damped vdW−QDO potential can accurately describe vdW interactions in dimers consisting of group II elements. Finally, we demonstrate the applicability of the atom-in-molecule vdW−QDO model for predicting accurate dispersion energies for molecular systems. The present work makes an important step toward constructing universal vdW potentials, which could benefit (bio)molecular computational studies.



Downloaded via 83.222.50.49 on October 4, 2025 at 12:25:51 (UTC).
See https://pubs.acs.org/sharingguidelines for options on how to legitimately share published articles.

INTRODUCTION

Van der Waals (vdW) forces play an indisputably important role in determining the structure and dynamics of many biomolecular, solid-state, and polymeric systems.[1−5] The accurate description of vdW interactions requires sophisticated quantum-mechanical treatment using the adiabatic-connection fluctuation−dissipation theorem (ACFDT) in density-functional theory or high-level quantum chemistry methods, such as coupled cluster or quantum Monte Carlo.[4,5] However, the prohibitive computational cost of these methods precludes their applicability to extended (bio)molecular systems. Therefore, practical simulations of large and complex systems are often done using classical force fields such as AMBER,[6] CHARMM,[7] or GROMACS.[8]

For the description of vdW forces, these popular force fields resort to the seminal Lennard-Jones (LJ)[9] (or an improved Buckingham[10]) potential as a practical shortcut. Two parameters, well depth D_e and equilibrium position R_e, fully specify the LJ potential. However, these parameters can be determined unambiguously only for relatively simple vdW-bonded systems, such as noble-gas dimers or crystals. Moreover, the LJ potential is notorious for its lack of flexibility and very limited quantitative accuracy.[11,12] On the other hand, the celebrated Tang−Toennies (TT) potentials[13−16] are derived from first principles and yield high accuracy for dimers including noble gases and group II elements. To achieve such an accuracy, the TT potentials employ 5 to 9 parameters depending on the exact flavor.[16] Setting these parameters requires knowledge of R_e and D_e for each vdW-bonded dimer,[13,15] which prevents a generalization of the TT models to the whole periodic table. Moreover, like the LJ potential, the most recent conformal Tang-Toennies-Sheng (TTS) potential[15] is prone to large errors for dispersion coefficients (see Figure 1a) despite its high accuracy close to equilibrium distances. Hence, a vdW potential combining wide transferability across the periodic table, high accuracy, and minimal parameterization is not yet available.

Here, we develop a universal conformal pairwise vdW potential, which can be parameterized for all chemical elements based solely on two nonbonded atomic properties—static dipole polarizability α_1 and dipole−dipole dispersion coefficient C_6. Our potential is consistently derived within the

Received: July 21, 2023
Revised: September 30, 2023
Accepted: October 5, 2023
Published: October 24, 2023



ACS Publications
© 2023 The Authors. Published by American Chemical Society

https://doi.org/10.1021/acs.jctc.3c00797
J. Chem. Theory Comput. 2023, 19, 7895−7907

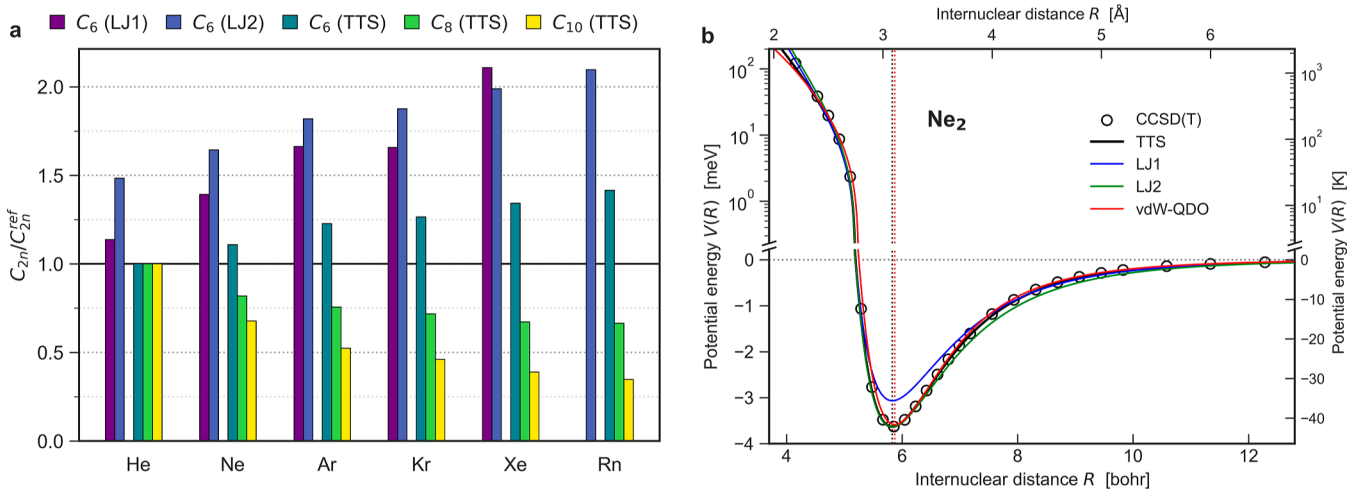


Figure 1. (a) Errors in the dispersion coefficients arising from the LJ and TTS potentials. The TTS dispersion coefficients are obtained as $C_{2n} = C_{2n}^{*} \times D_e R_e^{2n}$,[15] and the reference dispersion coefficients C_{2n}^{ref} are given in Table 1. (b) vdW−QDO potential for neon dimer benchmarked to the TTS potential and the reference CCSD(T) potential.[57] Vertical dotted lines indicate the equilibrium distance as predicted by the CCSD(T) (black) and vdW−QDO potential (red). For comparison, the LJ potentials in two different parameterizations (see our discussion in the text) are also displayed in blue and green.

Table 1. Reference Values of Static Dipole Polarizability α_1 (in a.u.), Dispersion Coefficients C_6, C_8, C_{10} (in a.u.), and Dimer Potential Well Parameters R_e (in bohr) and D_e (in meV) for Noble-Gas Dimers[a]

	α_1[66]	C_6[66]	C_8[67]	C_{10}[67]	R_e^{ref} (in Å)[15]	R_e (in Å)	D_e^{ref} (in K)[15]	D_e (in K)
He_2	1.38	1.46	14.123	183.79	5.608 (2.97)	5.35 (2.83)	0.948 (10.99)	1.634 (19.0)
Ne_2	2.67	6.38	90.265	1532.8	5.83 (3.09)	5.87 (3.11)	3.632 (42.15)	4.049 (47.0)
Ar_2	11.1	64.3	1621.5	49,033	7.11 (3.76)	7.20 (3.81)	12.319 (142.95)	12.00 (139.3)
Kr_2	16.8	129.6	4040	150,130	7.589 (4.02)	7.64 (4.04)	17.310 (200.87)	16.94 (196.6)
Xe_2	27.3	285.9	12,004	588,210	8.273 (4.38)	8.19 (4.33)	24.126 (279.97)	24.64 (285.9)
Rn_2	33.54	420.6*	19,263*	1,067,000*	8.37 (4.43)	8.43 (4.46)	34.885 (404.81)	30.38 (352.5)

[a]For R_e and D_e, the values in Å and Kelvin, respectively, are extra given in parentheses. Also, we compare their reference values (columns 5 and 7) to the predictions of eqs. 10 and 17 (columns 6 and 8). The values for C_6, C_8, and C_{10} labeled with the star (*) are taken from ref 13 instead of refs 66 and 67.

framework of the quantum Drude oscillator (QDO) model[17] using the Heitler−London perturbation theory,[18,19] and it is devoid of adjustable parameters. This is achieved by building connections between atomic scaling laws,[20−22] the microscopic law of corresponding states,[23−26] and symmetry-adapted perturbation theory (SAPT)[27,28] for intermolecular interactions. The derived exchange repulsion term in our potential obeys correct physical limits both at $R \to 0$ and $R \to \infty$, and the predicted C_6 dispersion coefficients are significantly more accurate compared to the other conformal LJ and TTS[15] potentials. The designed vdW−QDO potentials are twice as accurate as the LJ potentials when averaged over 15 noble-gas dimers. In addition, the vdW−QDO potential augmented by a damping function can accurately describe the binding curves of dimers consisting of (closed-shell) group II atoms. Moreover, the vdW−QDO potential can be applied to molecular systems, when coupled with the atom-in-molecule (AIM) approach.[29] We demonstrate this by accurately reproducing the dispersion energy for dispersion-dominated molecular dimers from the S66 × 8 data set.[30]

We derive the vdW potential in the QDO framework, which is a coarse-grained model for the electronic response[31−36] and proved to be accurate and insightful in many applications across various fields.[17,21,36−45] Within the QDO model, the response of valence electrons is described via a quasi-particle (drudon or Drude particle) with a negative charge $-q$ and mass μ, harmonically bound to a positively charged pseudonucleus of charge q with a characteristic frequency ω. Coupled QDOs are also extensively used in the development of vdW density functionals,[29,40,46−48] quantum mechanical,[17,36] and polarizable force fields[39,49−52] as well as recent machine learning force fields.[53,54]

The QDO model has already been used to build interatomic vdW potentials for water or noble-gas dimers and crystals.[17,36,38,39,55] However, within the corresponding studies, the repulsive term was added in an *ad hoc* manner, either by fitting Born−Mayer[10,56] exponents to *ab initio* repulsive walls[17,36,38,39] or by directly adding the Hartree−Fock exchange energy.[55] Therefore, such potentials cannot be generalized beyond the systems for which direct first-principles simulations are possible. In contrast, here, we suggest a consistent treatment of both Pauli (exchange) repulsion and vdW dispersion within the QDO framework. To our knowledge, this is the first vdW potential of such a type, which does not directly utilize the reference binding energy of dimers or the Hartree−Fock exchange energy curve but nevertheless provides relatively good accuracy.

RESULTS

Model Construction. The long-range vdW dispersion energy for two identical QDOs is given by the usual multipolar series[17,35]

https://doi.org/10.1021/acs.jctc.3c00797
J. Chem. Theory Comput. 2023, 19, 7895−7907

$$E_{\mathrm{disp}}(R) = -\frac{C_6}{R^6} - \frac{C_8}{R^8} - \frac{C_{10}}{R^{10}} - \dots \tag{1}$$

where the dispersion coefficients are related to the oscillator parameters via the closed-form expressions[17]

$$C_6 = \frac{3}{4}\hbar\omega\alpha_1^2 k_e^2, \qquad C_8 = \frac{5\hbar}{\mu\omega}C_6, \qquad C_{10} = \frac{245\hbar^2}{8(\mu\omega)^2}C_6 \tag{2}$$

where $\alpha_1 = q^2/\mu\omega^2$ is the QDO dipole polarizability and $k_e = 1/4\pi\varepsilon_0$. Tang and Toennies showed[13,14] that including the three leading dispersion terms is sufficient to obtain the accurate vdW potential. Therefore, we also truncate the series of eq 1 to the C_{10} term.

The exchange repulsion is introduced into the model according to refs 20 and 21, where multipole contributions to the exchange energy of a homonuclear dimer were derived by considering two identical drudons as bosons, assuming that they represent closed valence shells of atoms with zero total spin. Consequently, the total wave function of a dimer is represented by a symmetrized product

$$\Psi(\mathbf{r}_1, \mathbf{r}_2) = \frac{1}{\sqrt{2}}(\psi_A(\mathbf{r}_1)\psi_B(\mathbf{r}_2) + \psi_A(\mathbf{r}_2)\psi_B(\mathbf{r}_1)) \tag{3}$$

where $\psi_A(\mathbf{r}_1) = (\mu\omega/\pi\hbar)^{3/4} e^{-(\mu\omega/2\hbar)\mathbf{r}_1^2}$ and $\psi_B(\mathbf{r}_2) = (\mu\omega/\pi\hbar)^{3/4} e^{-(\mu\omega/2\hbar)(\mathbf{r}_2-\mathbf{R})^2}$ are, respectively, the ground-state wave functions of drudons centered at nuclei A and B separated by $\mathbf{R}$. Within the Heitler−London perturbation theory,[18,19] the exchange energy of two identical vdW-bonded QDOs for distances near equilibrium and larger is well approximated by the exchange integral[20]

$$E_{\mathrm{ex}} \approx J_{\mathrm{ex}} = \langle \psi_A(\mathbf{r}_1)\psi_B(\mathbf{r}_2)|\hat{V}_C|\psi_A(\mathbf{r}_2)\psi_B(\mathbf{r}_1)\rangle \tag{4}$$

The evaluation of eq 4 with the multipole expansion of Coulomb coupling $\hat{V}_C$ between the two QDOs results in multipole contributions to the exchange energy.[20,21] In dipole approximation, this yields

$$J_{\mathrm{ex}}^{(1)} = \frac{k_e q^2 S}{2R}, \qquad S = |\langle\psi_A|\psi_B\rangle|^2 = e^{-(\mu\omega/2\hbar)R^2} \tag{5}$$

where S is the overlap integral. Higher-order multipole contributions ($l > 1$) to the exchange repulsion energy $J_{\mathrm{ex}}^{(l)}$ have the same leading-term dependence on internuclear distance R, with the only difference in a proportionality coefficient, i.e., $J_{\mathrm{ex}}^{(l)} \propto k_e q^2 S/R$.[21] Therefore, we introduce an effective exchange repulsion energy as

$$E_{\mathrm{ex}}^{\mathrm{eff}} = A k_e q^2 S/R \tag{6}$$

with the proportionality coefficient A to be determined self-consistently, in what follows. In this way, we effectively include multipole contributions to all orders. Importantly, our $E_{\mathrm{ex}}^{\mathrm{eff}}$ has a $1/R$ dependence, which properly describes the infinite repulsive wall at short distances. Thus, in contrast to the Born−Mayer or Duman−Smirnov[58−60] functional forms for exchange repulsion possessing a finite value of E_{ex} at $R \to 0$, eq 6 is in agreement with the orbital overlap model for Pauli repulsion.[61,62] Moreover, our $E_{\mathrm{ex}}^{\mathrm{eff}}$ does not rely on empiricism as it explicitly depends only on the QDO parameters (*vide infra*), whereas the existing Pauli repulsion models require fitting to some *ab initio* data.[17,36,37,60,62−64]

In order to determine the coefficient A in eq 6, we employ the force balance condition at the equilibrium distance, $(-\nabla_R E_{\mathrm{ex}}^{\mathrm{eff}} - \nabla_R E_{\mathrm{disp}})|_{R=R_e} = 0$, which yields

$$A k_e q^2 \left[\frac{1}{R_e^2} + \frac{\mu\omega}{\hbar}\right] e^{-(\mu\omega/2\hbar)R_e^2} = \frac{6C_6}{R_e^7} + \frac{8C_8}{R_e^9} + \frac{10C_{10}}{R_e^{11}} \tag{7}$$

To evaluate the equilibrium distance R_e in our model, we use the quantum-mechanical relation between the atomic (static) dipole polarizability and vdW radius[20]

$$\alpha_1 = \Phi \times R_{\mathrm{vdW}}^7 \tag{8}$$

where the proportionality coefficient Φ is given by[22]

$$\Phi = (4\pi\varepsilon_0/a_0^4) \times \alpha_{\mathrm{fsc}}^{4/3} \tag{9}$$

with $\alpha_{\mathrm{fsc}} = e^2/4\pi\varepsilon_0\hbar c \approx 1/137.036$ as the fine-structure constant. The relation given by eqs 8 and 9 turned out to be valid for real atoms. Especially, it is very accurate for noble gases, where the mean absolute relative error (MARE) $\langle|R_{\mathrm{vdW}} - R_{\mathrm{vdW}}^{\mathrm{ref}}|/R_{\mathrm{vdW}}^{\mathrm{ref}}\rangle$ is about 1%.[20,22] Since by definition R_{vdW} is a half of the equilibrium distance R_e in a homonuclear vdW-bonded dimer,[20,65] accurate equilibrium distances can be obtained via

$$R_e = 2 \times R_{\mathrm{vdW}} = 2 \times (\alpha_1/\Phi)^{1/7} \tag{10}$$

With α_1 and C_6 being fixed, there are two unknown quantities in eq 7, A and $\mu\omega$, since C_8 and C_{10} are solely expressed in terms of C_6 and $\mu\omega$ via eq 2.

As shown in ref 45, the product $\mu\omega$ can be obtained from the force balance in the dipole approximation

$$\frac{k_e q^2}{2}\left[\frac{1}{R_e^2} + \frac{\mu\omega}{\hbar}\right] e^{-(\mu\omega/2\hbar)R_e^2} = \frac{6C_6}{R_e^7} \tag{11}$$

with R_e substituted from eq 10. The solution of this transcendental equation allows us to determine the three oscillator parameters $\{q, \mu, \omega\}$ given only $\{\alpha_1, C_6\}$. Let us call this parameterization scheme vdW−QDO, similar to the recently suggested optimized quantum Drude oscillator (QDO) scheme.[45] The details of the procedure and the corresponding values of $\{q, \mu, \omega\}$ can be found in the Supporting Information.

Solving eqs 11 and 7 together, one can obtain

$$A = \frac{1}{2} + \frac{2C_8}{3C_6R_e^2} + \frac{5C_{10}}{6C_6R_e^4} \tag{12}$$

and the total vdW potential

$$V_{\mathrm{QDO}} = A\frac{k_e q^2}{R} e^{-(\gamma R)^2/2} - \sum_{n=3}^{5}\frac{C_{2n}}{R^{2n}}, \qquad \gamma = \sqrt{\mu\omega/\hbar} \tag{13}$$

The vdW−QDO potential for neon is displayed by the red curve in Figure 1b, which shows excellent agreement with the TTS potential[15] as well as with the CCSD(T) calculations[57] across the whole range of distances from $0.7R_e$ (~4 bohr) to infinity. Inclusion of C_8 and C_{10} dispersion coefficients together with the suggested approach to treat exchange repulsion energy allows us to predict the correct depth and shape of the potential without losing the accuracy in predicting the equilibrium distance, which is inherited from the dipole approximation. In addition, we compare our potential to the LJ potential, for which we use two different parameterizations:

https://doi.org/10.1021/acs.jctc.3c00797
J. Chem. Theory Comput. 2023, 19, 7895−7907

LJ1 derived from thermodynamical properties and LJ2 designed to reproduce reference values of R_e and D_e (see the Supporting Information for more details). We note that the present vdW−QDO potential (eq 13) performs accurately over the whole range of distances, whereas the LJ1 potential (blue curve in Figure 1b) underestimates the energy in the potential minimum region and the LJ2 potential overestimates the long-range energy (green curve), although both being reasonably accurate in the repulsive region. This imbalance and lack of flexibility of the LJ potential, which is observed for all noble gases, is one of the main issues limiting its quantitative predictive power.[11,12] Moreover, the LJ potential severely overestimates the C_6 coefficient (Figure 1a), which is responsible for the correct long-range energy. The proposed vdW−QDO potential overcomes these difficulties without increasing the number of parameters. Moreover, our potential recovers correct bonding behavior using only a free atom property α_1 and the asymptotic interaction parameter C_6, which do not contain information about the interaction between atoms at short distances.

Application to Noble-Gas Dimers. With the accurate Ne_2 potential curve in hand, its counterparts for all other noble-gas dimers can be derived using the conformality of their potentials,[15,68,69] which is a microscopic manifestation of the law of corresponding states.[23−25] Namely, for the vdW potential of other noble-gas dimers, we write

$$V_{QDO}(R) = D_e U^{Ne}_{QDO}(x), \qquad x = R/R_e \tag{14}$$

where $U^{Ne}_{QDO}(x) = V^{Ne}_{QDO}(xR^{Ne}_e)/V^{Ne}_{QDO}(R^{Ne}_e)$ is the dimensionless potential (shape) of the Ne_2 dimer

$$U^{Ne}_{QDO}(x) = \frac{A^*}{x} e^{-(\gamma^* x)^2/2} - \sum_{n=3}^{5} \frac{C^*_{2n}}{x^{2n}} \tag{15}$$

with the numerical values of the starred (unitless) parameters and their definitions presented in Table 2.

Thus, only R_e and D_e for every dimer are required to obtain their vdW potential. For R_e, the accurate scaling law (eq 10) is already established, whereas an analogous scaling law for D_e of noble-gas dimers is not yet known. Substituting $R = R_e$ to eq 13 and using eq 7 to eliminate $Ak_e q^2 e^{-(\gamma R)^2/2}/R$ yields

Table 2. Dimensionless Parameters in eq 15[a]

parameter	definition	numerical value
A^*	$Ak_e q^2/R_e D_e$	1508.917
γ^*	$R_e\sqrt{\mu\omega/\hbar}$	3.912
C_6^*	$C_6/D_e R_e^6$	1.1779
C_8^*	$5C_6/D_e R_e^6(\gamma^*)^2$	0.3848
C_{10}^*	$245C_6/8D_e R_e^6(\gamma^*)^4$	0.1540

[a]The neon dimer parameters used in the second column are $D_e(Ne_2)$ = 3.586 meV = 13.178 × 10^{-5} a.u. [eq 16] and $R_e(Ne_2)$ = 5.875 bohr [eq. 10]. The QDO parameters for the Ne_2 dimer are q = 1.18865, μ = 0.37164, and ω = 1.19326 (all in a.u.).

$$D_e = -V^{Ne}_{QDO}(R^{Ne}_e) = \frac{C_6}{R_e^6}\left(1 - \frac{\beta - 5}{\beta(1+\beta)} - \frac{40}{\beta(1+\beta)} + \frac{245}{8\beta^2} - \frac{2450}{8\beta^2(1+\beta)}\right) \tag{16}$$

with $\beta = \frac{\mu\omega}{\hbar}R_e^2 = (\gamma^*)^2$. Analyzing reference CCSD(T) data for D_e from ref 15, we found that eq 16 truncated at the first two terms can accurately predict D_e for all noble-gas dimers

$$D_e \approx \frac{C_6}{R_e^6}\left(1 - \frac{\beta - 5}{\beta(1+\beta)}\right) \tag{17}$$

In Figure 2, the D_e values by eq 17 are compared to the reference CCSD(T) data. The bar chart shows that eq 17 is accurate for homo- and heteronuclear dimers of He−Xe with all errors below 1 meV. For dimers with Rn, the error is larger, with Rn_2 being underbound by 4.5 meV or 13%. The larger errors for Rn dimers likely stem from the fact that the reference coupled-cluster calculation[76] is less reliable than the corresponding calculations for the lighter dimers He_2−Xe_2.[57,70−73] For example, the D_e of the Xe_2 dimer reported in ref 76 is by 7.5% larger than the one of ref 73, which is a state-of-the-art calculation. Thus, a similar or even larger overestimation of D_e should be expected for Rn_2,[76] where relativistic effects are more pronounced. Accounting for that, the estimated error of eq 17 for Rn_2 would not exceed 5.5%. We conclude that the suggested scaling law (eq 17) allows one to accurately evaluate D_e for all noble-gas dimers given only $\{\alpha_1, C_6\}$ without involving any adjustable parameters.

To extend the developed potential to heteronuclear dimers, combination rules for the potential parameters can be used. The simplest ones are given by

$$R_e^{AB} = \frac{(R_e^A + R_e^B)}{2}, \qquad D_e^{AB} = \sqrt{D_e^A D_e^B} \tag{18}$$

and known as the Lorentz−Berthelot rules, which are often used for the LJ potential and implemented in many molecular simulation packages.[6−8] However, the Lorentz−Berthelot rules are not accurate.[20,77−79] Therefore, instead of mixing R_e and

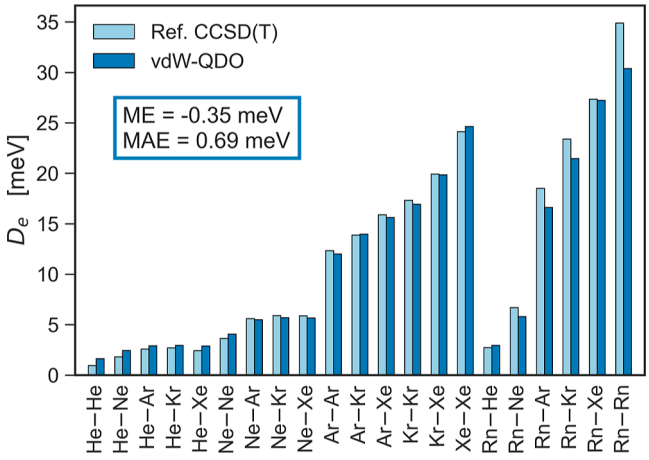


Figure 2. Potential well depth D_e by eq 17 compared to the reference CCSD(T) values[15] for 21 noble-gas dimers. Mean error (ME) and mean absolute error (MAE) are displayed.

https://doi.org/10.1021/acs.jctc.3c00797
J. Chem. Theory Comput. 2023, 19, 7895−7907

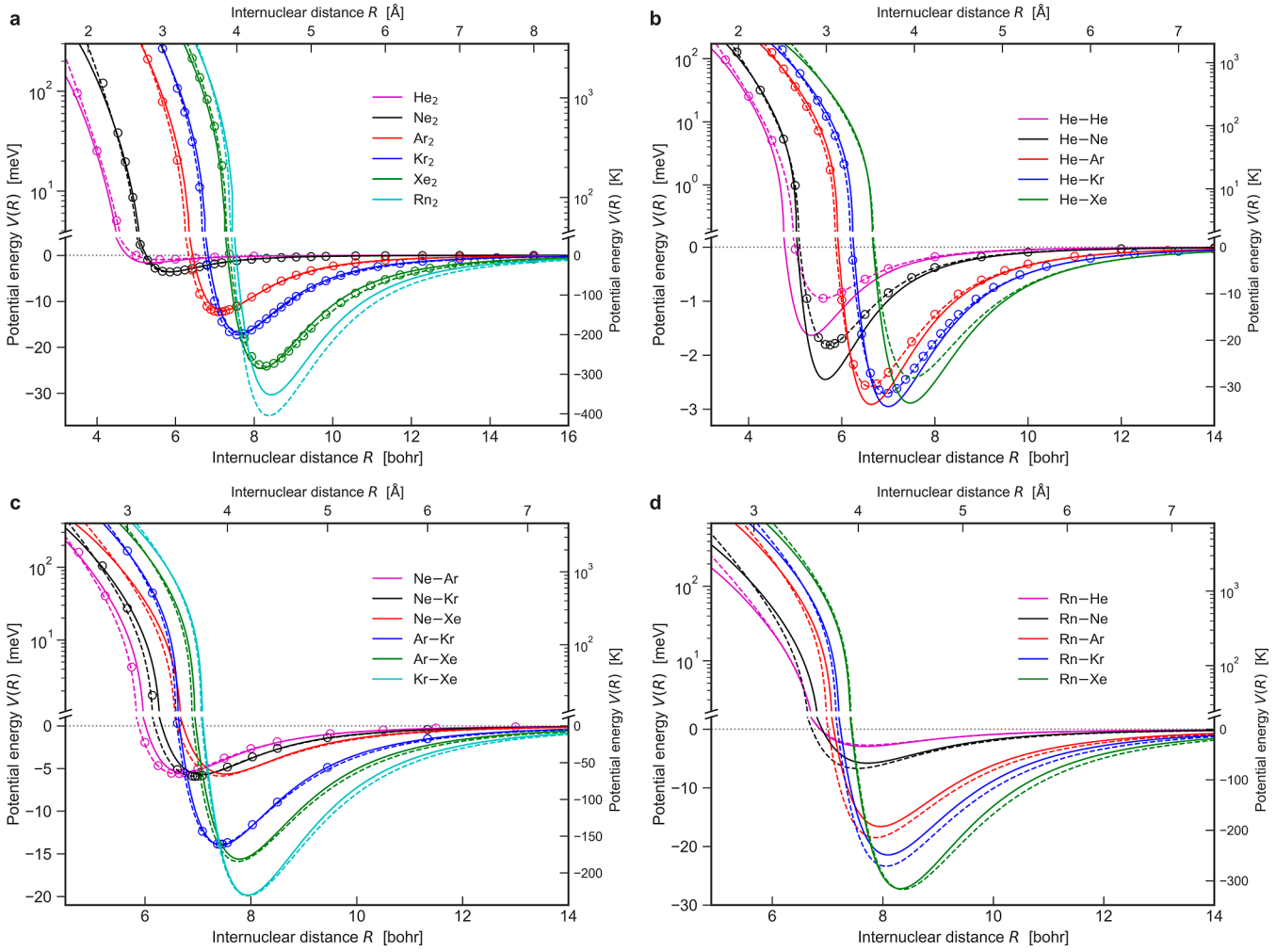


Figure 3. vdW−QDO potentials (solid lines) for (a) homonuclear and (b−d) heteronuclear noble-gas dimers benchmarked to the TTS potential[15] (dashed lines) and the reference CCSD(T) calculations (circles).[57,70−75]

D_e, we use mixing rules for α_1 and C_6 since our potential is fully parameterized by these two quantities. With the effective mixed values $\{\alpha_1^{AB}, C_6^{AB}\}$, we can set three oscillator parameters $\{q, \mu, \omega\}$ through the same vdW−QDO parameterization procedure as for homonuclear dimers, which is described in the Supporting Information. By doing so, even the heteronuclear dimer AB is effectively represented by two identical oscillators, which still allows us to apply the formalism for exchange repulsion, eqs 3 and 4, developed for homonuclear dimers. For the C_6 dispersion coefficient, the very accurate combination rule arising from the London formula is already well-known[13,80]

$$C_6^{AB} = \frac{2\alpha_1^A \alpha_1^B C_6^A C_6^B}{C_6^A(\alpha_1^B)^2 + C_6^B(\alpha_1^A)^2} \tag{19}$$

To combine polarizabilities, we employ the robust mixing rule for vdW radii which was established in ref 20, where it was shown that accurate equilibrium distances in noble-gas dimers (MARE = 1%) are delivered by

$$R_e^{AB} = 2 \times \Phi^{-1/7}[(\alpha_1^A + \alpha_1^B)/2]^{1/7} \tag{20}$$

similar to the homonuclear case (eq 8). Thus, the effective polarizability α_1^{AB} can be simply represented by

$$\alpha_1^{AB} = (\alpha_1^A + \alpha_1^B)/2 \tag{21}$$

Thereby, combining eqs 14, 15, 17, 19, and 21 with the vdW−OQDO parameterization scheme (see the Supporting Information), we obtain vdW−QDO potentials for all 21 noble-gas dimers. They are shown in Figure 3 with excellent agreement to both TTS potential and reference CCSD(T) calculations for homo- and heteronuclear dimers of Ne, Ar, Kr, and Xe on panels (a) and (c), as well as for He−Ar, He−Kr (b), and Rn−Xe (d). The other Rn dimers are challenging for our model due to the discrepancies in D_e, as discussed above. In the case of He dimers, to a large extent the error is caused by the underestimated R_e of He_2, with 5.35 bohr predicted by eq 10 against the reference value of 5.608 bohr.[70] In addition, the actual error in potential for He dimers is small in magnitude (despite being seemingly large visually due to the scale of the y-axis in Figure 3b).

To evaluate the accuracy of our potential quantitatively, we introduce the normalized area difference metric Δ_S between tested and reference potentials as

$$\Delta_S = \frac{1}{R_e D_e} \int_{0.8R_e}^{2.0R_e} |V_{ref}(R) - V_{test}(R)|\, dR \tag{22}$$

The essential physical meaning of Δ_S is illustrated in Figure 4b which shows that this single unitless number represents a

https://doi.org/10.1021/acs.jctc.3c00797
J. Chem. Theory Comput. 2023, 19, 7895−7907

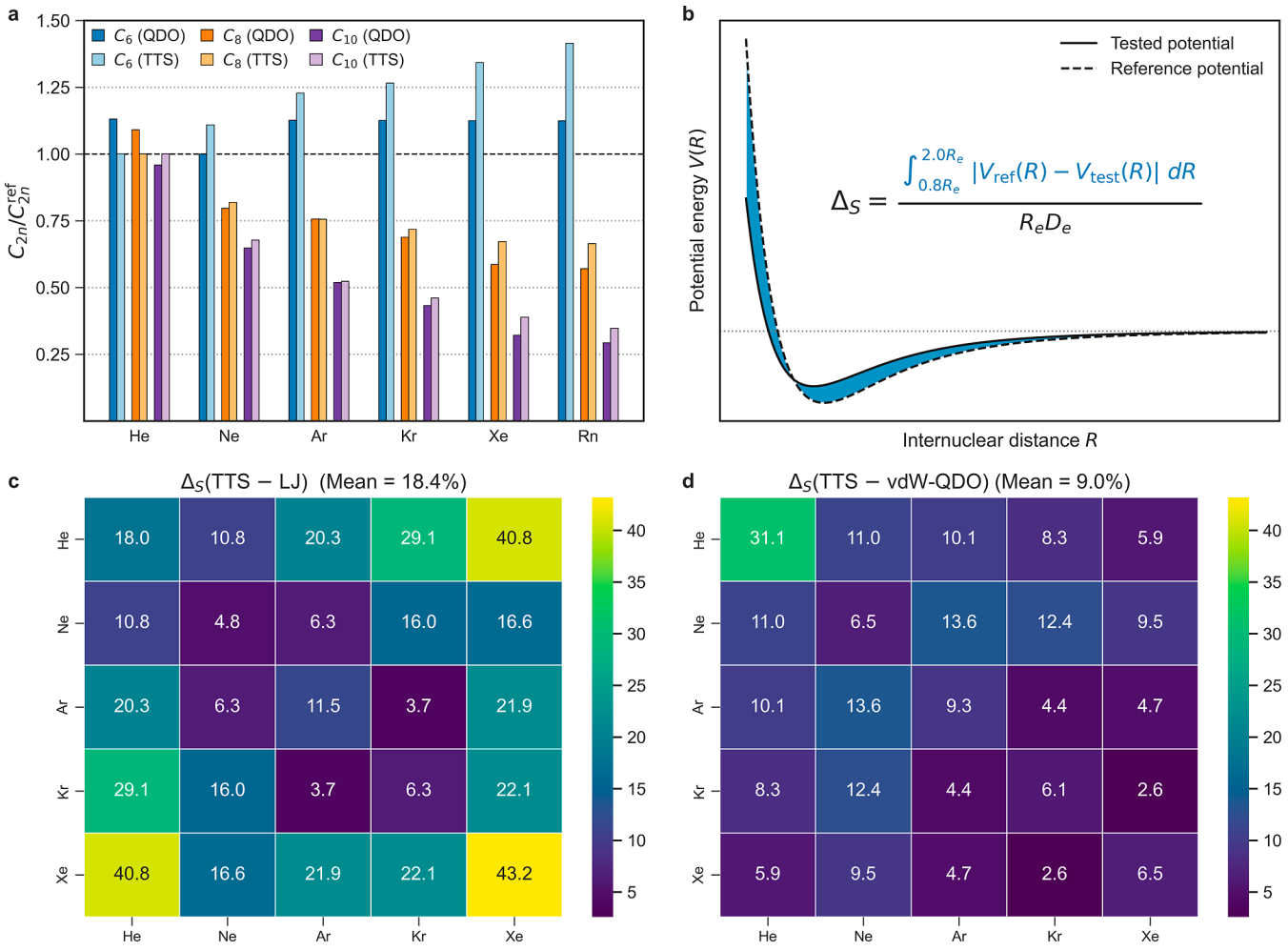


Figure 4. (a) Errors in dispersion coefficients predicted by vdW−QDO (dark colors) and TTS (light colors) potentials. (b) Schematic illustration of the Δ_S metric calculation. (c) Heatmaps showing Δ_S (in %) for LJ1 (left) and vdW−QDO (right) potentials with respect to the reference TTS potential. The left and right colorbars have the same scale.

measure of the difference between tested and reference potentials. The integration limits are set to $0.8R_e$ and $2.0R_e$ in order to evaluate accuracy close to the minimum region, whereas the long-range accuracy can be evaluated separately in terms of dispersion coefficients. Previously, Δ-gauge was used in benchmarks of various density-functional codes in calculations of equations of state for solids.[81,82] The TTS potential[15] was chosen as the reference potential, and we benchmark the vdW−QDO and LJ1 potentials with respect to it (a similar benchmark for LJ2 can be found in the Supporting Information). The computed Δ_S-matrices for 15 He−Xe dimers are displayed in Figure 4c−d (Rn dimers are omitted since there are no LJ parameters for Rn available in the literature). We note that the vdW−QDO potential has twice better accuracy than the LJ one with $\langle\Delta_S^{QDO}\rangle$ = 9.0% compared to $\langle\Delta_S^{LJ1}\rangle$ = 18.4% and $\langle\Delta_S^{LJ2}\rangle$ = 17.3% when averaged over 15 dimers. Helium is the obvious outlier for vdW−QDO with the highest Δ_S = 31.1%, whereas for all other dimers, Δ_S is below 13.6%. In contrast, the LJ potential shows much broader variations in Δ_S spanning from 3.7% for Ar−Kr to 43.2% for Xe_2. Although the LJ potential shows better Δ_S values than vdW−QDO for some of the dimers (He_2, Ne_2, He−Ne, Ne−Ar, and Ar−Kr), overall the performance of the vdW−QDO potential is more accurate and robust. Generally, Figure 4 supports the above conclusions about the accuracy of the vdW−QDO potential based on Figure 3. We note that the predictions of LJ potential become worse for heteronuclear dimers composed of small and large atoms (e.g., He−Ar, He−Kr, and Ne−Kr) than for atoms with a relatively close size (Ne−Ar, Ar−Kr) (Figure 4c). In contrast, the evenly accurate predictions of the vdW−QDO model (Figure 4d) suggest that the combination rules eqs 19 and 21 employed in this work are more accurate and robust than the Lorentz−Berthelot rules (eq 18).

To evaluate the quality of the potentials in the long-range limit, in Figure 4a we compare the dispersion coefficients predicted by vdW−QDO and TTS potentials to the reference *ab initio* values (Table 1). Such a comparison is fair, since both potentials are built as conformal ones, unlike the earlier TT-2003 potentials,[13] which directly utilize reference C_{2n} coefficients for every element being therefore not strictly conformal. To recover the TTS dispersion coefficients, we used the reported scaling law $C_{2n} = C_{2n}^* \times D_e R_e^{2n}$ with C_6^* = 1.3499, C_8^* = 0.4147, and C_{10}^* = 0.1716.[15] For vdW−QDO dispersion coefficients, from eqs 14, 15 and 17, one can obtain

$$C_{2n} = C_{2n}^* \times \frac{C_6}{R_e^{2n-6}}\left[1 - \frac{\beta - 5}{\beta(\beta + 1)}\right] \quad (23)$$

https://doi.org/10.1021/acs.jctc.3c00797
J. Chem. Theory Comput. 2023, 19, 7895−7907

where $C_6^* = 1.1779$, $C_8^* = 0.3848$, and $C_{10}^* = 0.1540$ (see Table 2). We found that both potentials severely underestimate C_8 and C_{10} and demonstrate a similar magnitude of these errors increasing with the atomic number. However, for C_6, the vdW−QDO potential performs much better, showing a homogeneous overestimate of 12−13%, whereas the TTS potential again possesses an increasing magnitude of error, reaching its maximum of 41% for Rn. While C_8 and C_{10} are important to deliver accurate potential near the equilibrium, in the asymptotic limit the quality of the potential is fully determined by the leading C_6 coefficient. Therefore, we can conclude that our conformal vdW−QDO potential shows physically more reasonable long-range behavior than the conformal TTS potential.

In contrast to the TTS potentials,[13,15] the above vdW−QDO model does not employ any damping of the dispersion energy. However, for noble-gas dimers, the damping of the dispersion energy is not essential, and interatomic vdW potential can be effectively described even without a damping function, as was shown above. This provides additional reasoning why the scaling law for vdW radius (eq 8), which was originally derived without considering dispersion damping,[20] works so well. To check the effect of the damping function on the results, we derived the damped vdW−QDO potential, where the QDO damping function reads

$$f_{2n}(z) = 1 - e^{-z}\sum_{k=0}^{n}\frac{z^k}{k!}, \qquad z = \frac{(\gamma R)^2}{2} \tag{24}$$

It was found that for noble-gas dimers the obtained damped vdW−QDO potential curves are practically the same as the undamped ones within the considered range of distances (see Figure S2 in the Supporting Information). Interestingly, the damping function (eq 24) differs from the TTS damping function[83] just in the upper summation limit [for the Tang−Toennies(TT) it is $2n$] and in the physical meaning of the unitless variable ($z = bR$ for the TT damping function, with b stemming from the Born−Mayer repulsion term Ae^{-bR}). Note that, due to the distinct form of the Pauli repulsion in the vdW−QDO and TT models, the QDO damping function contains only even powers of R up to $2n$ (see the derivation of the QDO damping function and more detailed discussion in the Supporting Information).

We also observe that for both the TT and vdW−QDO models exchange repulsion and dispersion terms separately do not agree with their SAPT counterparts, whereas the total potentials show very close agreement with the sum of the SAPT terms (see the Supporting Information). This finding is in line with the statement of ref 60 that the generalized Heitler−London theory delivers a more compact expansion of interaction energy than the SAPT.

Application to Group II Dimers. Another class of vdW systems where TTS potentials work well consists of Me_2 dimers, with Me = Mg, Ca, Sr, Ba, Zn, Cd, and Hg. Although such systems are not purely vdW-bonded, it was demonstrated that their interatomic potentials can be also well described by the TT potential.[14,84−89] Moreover, the potentials of the group II dimers also obey the principle of corresponding states, albeit the underlying potential shape is distinct from that of noble-gas dimers.[86−88] The only exception is the Be−Be dimer, which has been a longstanding puzzle for quantum chemistry. The potential curve of Be_2 has a remarkably different shape in the long-range region, compared to other alkaline-earth elements.[87] Since this dimer does not obey the principle of corresponding states, it is excluded from our consideration here. In what follows, we show that the vdW−QDO potential is also capable of describing the potential curves of the group II dimers upon several modifications.

First, in contrast to noble gases, for Me_2 dimers, the damping function (eq 24) cannot be omitted due to much larger polarizabilities and hence dispersion coefficients than those of noble gases (see Table 3). As a result, without the damping function, a pronounced divergence of the vdW−QDO potential would already occur at near-equilibrium distances. Second, the scaling laws of eqs 10 and 17 are not so accurate for the group II dimers since the bonding in Me_2 is not purely of vdW type.[86,87] Therefore, the reference values of R_e and D_e (Table 3) were used for the vdW−QDO potential.

Following Tang *et al.*,[87] we choose the strontium (Sr_2) dimer as the reference system to get the shape of the potential curve and then rescale it onto other dimers. Similar to the case of noble gases, the vdW−QDO potential shape for the Sr_2 dimer was derived as (see the Supporting Information)

$$U_{\mathrm{QDO}}^{\mathrm{Sr}}(x) = \frac{A_d^*}{x}e^{-(\gamma^* x)^2/2} - \sum_{n=3}^{5} f_{2n}(\gamma^* x)\frac{C_{2n}^*}{x^{2n}} \tag{25}$$

with the numerical values of its parameters presented in Table 4. The QDO parameters $\{q, \mu, \omega\}$ for the Sr_2 dimer were set using α_1, C_6, and R_e following the damped vdW−OQDO procedure, as explained in the Supporting Information. Altogether, the three physical quantities are employed to parameterize the vdW−QDO potential for Sr_2, compared to the five $\{R_e, D_e, C_6, C_8, \text{and } C_{10}\}$ in the case of the TT potential.[87] For other Me_2 dimers, we need only R_e and D_e from Table 3 to perform the rescaling

$$V_{\mathrm{QDO}}(R) = D_e U_{\mathrm{QDO}}^{\mathrm{Sr}}(x), \qquad x = R/R_e \tag{26}$$

The results in Figure 5 show that vdW−QDO potentials are in excellent agreement with both *ab initio* and experimentally derived potentials (when they are available). This is a remarkable result since the binding energies of group II dimers are up to 5 times larger than those of the heaviest noble gases. Furthermore, the shape of their potentials is distinct to the one of noble gases (Figure 6). Thus, the vdW−QDO functional form is robust and well-suited to describe vdW potentials across various types of systems. In contrast, the LJ

Table 3. Reference *Ab Initio* Values of the Dipole Polarizability α_1 (in a.u.), Dipolar Dispersion Coefficient C_6 (in a.u.), and Dimer Potential Well Parameters R_e (in bohr) and D_e (in meV) of the Group II Dimers[a]

	α_1	C_6	R_e (in Å)	D_e (in K)
Mg_2	71.3[b]	627[b]	7.35 (3.89)[c]	53.81 (624.4)[c]
Ca_2	157.1[b]	2121[b]	8.13 (4.30)[c]	130.18 (1511)[c]
Sr_2	197.2[b]	3103[b]	8.88 (4.70)[c]	129.69 (1505)[c]
Ba_2	273.5[b]	5160[b]	9.43 (4.99)[c]	169.36 (1965)[c]
Zn_2	38.67[d]	359[e]	7.23 (3.83)[f]	28.64 (332.4)[f]
Cd_2	46[d]	686[e]	7.32 (3.87)[f]	40.91 (474.8)[f]
Hg_2	33.9[d]	392[e]	6.95 (3.68)[g]	48.60 (564.0)[g]

[a]For R_e and D_e, the values in Å and Kelvin, respectively, are extra given in parentheses. The used data sources are the following. [b]Reference 90. [c]Reference 91. [d]Reference 92. [e]Reference 88. [f]Reference 93. [g]Reference 94.

https://doi.org/10.1021/acs.jctc.3c00797
J. Chem. Theory Comput. 2023, 19, 7895−7907

Table 4. Dimensionless Parameters in eq 25[a]

parameter	definition	numerical value
A_d^*	$A_d k_e q^2 / R_e D_e$	58.051
γ^*	$R_e\sqrt{\mu\omega/\hbar}$	2.992
C_6^*	$C_6/D_e R_e^6$	1.6209
C_8^*	$5C_6/D_e R_e^6(\gamma^*)^2$	0.9053
C_{10}^*	$245C_6/8D_e R_e^6(\gamma^*)^4$	0.6194

[a]The strontium dimer parameters used in the second column are $D_e(Sr_2)$ = 129.7 meV = 4.766 × 10^{-3} a.u. and $R_e(Sr_2)$ = 8.88 bohr.[91] The QDO parameters for the Sr_2 dimer are q = 1.5433, μ = 1.0671, and ω = 0.1064 (all in a.u.).

potential cannot be employed to describe group II dimers with any combination of parameters since its energy well is too narrow for such binding curves (Figure 6).

Application to Molecular Dimers. Finally, we can show that the developed vdW−QDO potential is also applicable to molecular systems, with an example of eight dispersion-dominated molecular dimers from the S66 × 8 benchmark data set.[30] They are hydrocarbons, including benzene as well as aliphatic and cyclic molecules (see the list in the Supporting Information). Such systems were chosen to diminish an influence of the electrostatic term not included in the current vdW−QDO potential.

We compute the energy of the vdW interaction between molecules A and B at the given intermolecular separation as

$$V_{QDO}^{vdW}(A,B) = V_{QDO}^{exc} + V_{QDO}^{disp} = \sum_{i\in A}\sum_{j\in B} V_{QDO}^{ij}(R_{ij}) \quad (27)$$

where summation goes over the atoms i and j of the molecules A and B, respectively, and R_{ij} is the interatomic distance. Interaction energy between a pair (i, j) is given by the damped vdW−QDO potential

$$V_{QDO}^{ij}(R_{ij}) = A_d\frac{k_e q^2}{R_{ij}} e^{-(\gamma R_{ij})^2/2} - \sum_{n=3}^{5} f_{2n}(\gamma R_{ij})\frac{C_{2n}}{R_{ij}^{2n}} \quad (28)$$

To set the QDO parameters $\{q, \mu, \omega\}$, we apply the vdW−OQDO procedure (see the Supporting Information) coupled with the AIM approach to each pair of atoms (i, j). Following

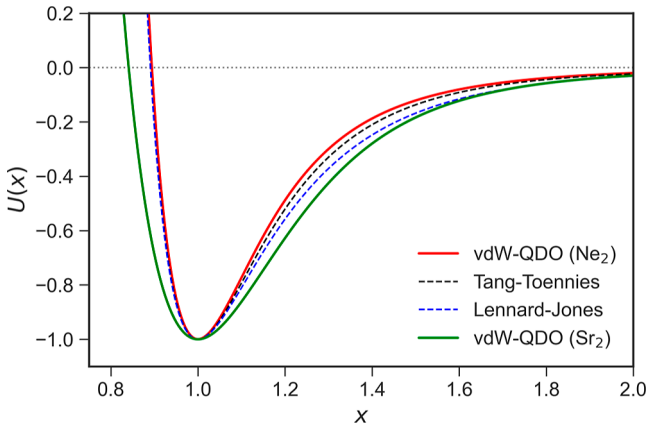


Figure 6. Dimensionless shapes of the vdW−QDO potential curves for Ne_2 (red) and Sr_2 (green) compared with the shapes of the LJ (dashed blue) and TTS (dashed black) potentials.

the Tkatchenko−Scheffler (TS) method,[29] the AIM polarizabilities and dispersion coefficients are defined by

$$\alpha_{1,i}^{AIM} = \alpha_{1,i}^{free}\left(\frac{V_i^{AIM}}{V_i^{free}}\right), \qquad C_{6,i}^{AIM} = C_{6,i}^{free}\left(\frac{V_i^{AIM}}{V_i^{free}}\right)^2 \quad (29)$$

where V_i^{free} and V_i^{AIM} are the corresponding Hirshfeld volumes. To compute them, single-point density-functional theory (DFT-PBE0)[98,99] calculations for every dimer were performed at their equilibrium geometry. Then, the effective polarizability α_1^{ij} and dispersion coefficient C_6^{ij} for a pair (i, j) were defined using the combination rules of eqs 19 and 21. Finally, the vdW−OQDO parameterization procedure (see the Supporting Information) was applied to map $\{\alpha_1^{ij}, C_6^{ij}\}$ onto $\{q, \mu, \omega\}$. After performing pairwise summation in eq 27 and repeating the whole procedure for all 8 intermolecular separations, the vdW−QDO interaction curves for dimers are obtained and compared to the reference CCSD(T) interaction curves.[30] For comparison, interaction energies of dimers at PBE0 + TS,[29] PBE0 + many-body dispersion (MBD),[40] and density functional tight-binding (DFTB3)[100] + MBD levels of theory were also calculated. All DFT calculations in this work were

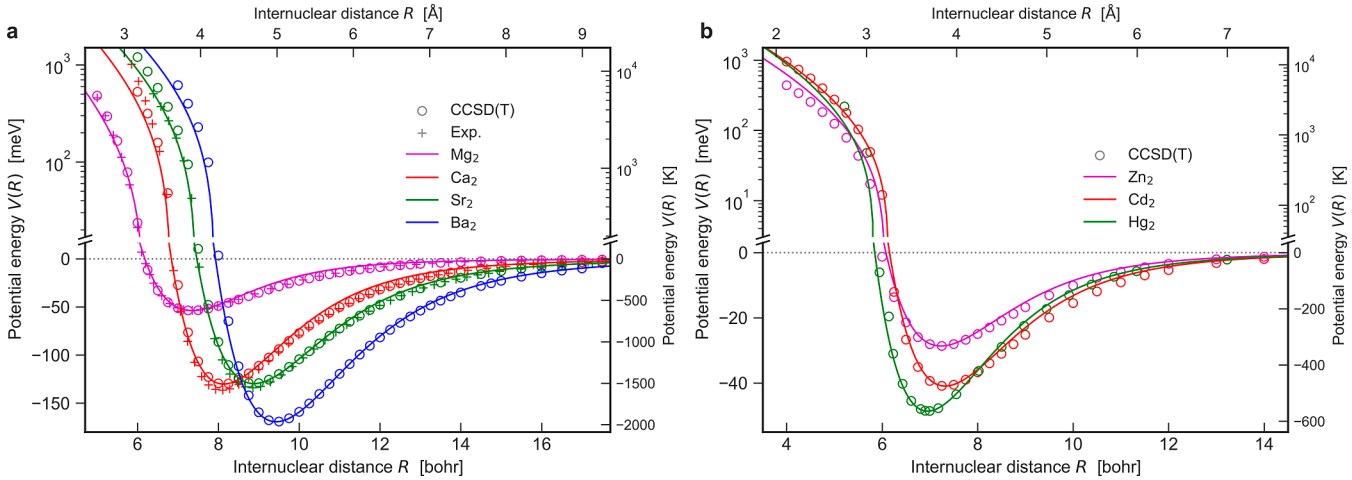


Figure 5. Interatomic potentials of (a) Mg_2, Ca_2, Sr_2, and Ba_2 and of (b) Zn_2, Cd_2, and Hg_2 dimers. The vdW−QDO potentials are shown by solid lines, circles mark coupled-cluster calculations,[91,93,94] and crosses display experimental potential curves.[95−97]

https://doi.org/10.1021/acs.jctc.3c00797
J. Chem. Theory Comput. 2023, 19, 7895−7907

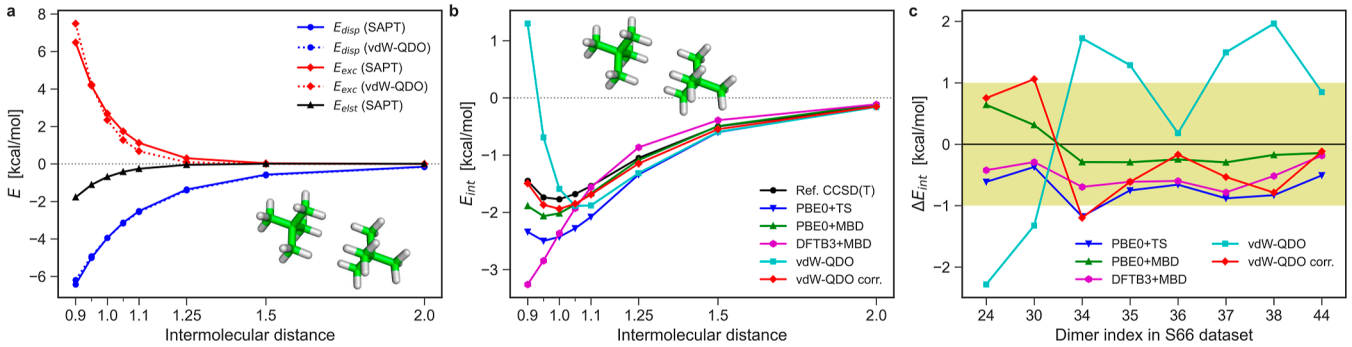


Figure 7. (a) Dispersion (blue) and exchange (red) contributions to the interaction energy of neopentane dimer (shown as inset) calculated by SAPT−DFT[102] (solid lines) and the damped vdW−QDO potential of eq 27 (dotted lines). In addition, the electrostatic term from SAPT−DFT is displayed in black. (b) Binding energy curves of neopentane dimer as calculated by different methods: CCSD(T)[30] (black); PBE0 + TS (blue) and PBE0 + MBD (green); DFTB3 + MBD (magenta); damped vdW−QDO potential (cyan); SAPT-corrected vdW−QDO potential (eq 30) (red). (c) Errors in the interaction energy of eight dispersion-dominated dimers for the five methods considered. Yellow filling depicts the "chemical accuracy" region of ±1 kcal/mol error.

performed using FHI-aims code[101] with the "tight" atomic basis sets.

We showcase the obtained results with an example of a neopentane dimer (Figure 7b). One can see that PBE0 + TS overbinds the neopentane dimer significantly and underestimates the equilibrium separation by 5%. Inclusion of many-body effects at the PBE0 + MBD level improves the results of PBE0 + TS for energy, but the predicted equilibrium separation is still 95% of the reference value. On the other hand, the DFTB3 + MBD method clearly lacks repulsion and attraction at short-range and long-range distances, respectively, although at the equilibrium distance the two errors largely cancel each other. As for the vdW−QDO potential, we note that the minimum of the intermolecular interaction curve is very close to the reference CCSD(T) energy, although our method overestimates the equilibrium separation by 10%. When considering the overall interaction curve, however, the vdW−QDO potential deviates significantly from the reference, being too repulsive at shorter distances. These conclusions remain valid also for the other seven dimers, as supported by the corresponding results in the Supporting Information.

To get insights into such a behavior, we compared the exchange and dispersion terms in vdW−QDO potential (eq 27) to their counterparts from SAPT−DFT calculations[102] (see Figure 7a). The dispersion part of the vdW−QDO potential provides excellent agreement with $E_{disp}^{(2)}$ from SAPT−DFT, which illustrates the well-known fact that vdW dispersion interaction between small molecules can be effectively described by a pairwise potential, despite being essentially many-body in its nature.[4,40,103] In contrast, for the vdW−QDO exchange repulsion term we observe a noticeable deviation from the $E_{exc}^{(1)}$ contribution of SAPT−DFT. This might indicate that exchange repulsion between molecules is not accurately described by the commonly used pairwise approach and hence exchange repulsion requires many-body treatment as well.[104]

SAPT−DFT calculations[102] also indicate that electrostatic contributions are small but not negligible even for dispersion-dominated dimers (Figures 7a and S6−S8 in the Supporting Information). To check a possible effect of the inclusion of accurate many-body exchange and electrostatic interactions on our results, we consider the corrected vdW−QDO potential, where the first-order SAPT−DFT energy was added to the dispersion energy from the vdW−QDO model

$$V_{QDO}^{corr}(A, B) = E_{elst}^{(1)} + E_{exc}^{(1)} + V_{QDO}^{disp} \quad (30)$$

This approach is similar to the Hartree−Fock plus dispersion plus first-order correlation [HFDc$^{(1)}$] scheme of Podeszwa *et al.*[105] with the important difference that here the dispersion energy is calculated from the QDO model, whereas in the HFDc$^{(1)}$ method, this energy is computed from SAPT. The corrected vdW−QDO curve in Figure 7b delivers a much better description of the interaction energy than the original vdW−QDO method. Notably, at larger distances, V_{QDO}^{corr} also shows a good agreement with PBE0 + MBD energy.

The overall statistics for the eight molecular dimers is shown in Figure 7c in terms of the error in the equilibrium energy obtained by five methods with respect to the reference CCSD(T) values.[30] Purely analytical vdW−QDO predictions are scattered within the 2 kcal/mol range, which is remarkable considering the approximations made in the model. Including the first-order SAPT energy reduces errors by roughly 1 kcal/mol (chemical accuracy).

This test demonstrates that the vdW−QDO approach is not limited to atomic dimers and can be generalized to molecular complexes, although in that case, the accuracy is currently lower. Nevertheless, considering the approximations made, the fact that the vdW−QDO method (even without SAPT corrections) properly predicts binding of the considered weakly bound molecular complexes from a set of AIM quantities (α_1 and C_6) is already reassuring.

SUMMARY AND OUTLOOK

We developed a universal pairwise vdW potential devoid of empiricism and parameterized by only two atomic nonbonded parameters. The developed vdW−QDO potential combines the strengths of the LJ and TTS models. Similarly to the former, the vdW−QDO potential is fully determined by only two parameters. At the same time, our potential is comparable in accuracy to the TTS potential for noble-gas dimers, being twice as accurate as the LJ one. Moreover, the vdW−QDO potential has advantages that are present neither in LJ nor in TTS models. First, the two parameters $\{\alpha_1, C_6\}$ are readily available for the whole periodic table,[66,92] being computed by highly accurate *ab initio* methods. This makes our potential widely applicable, as demonstrated for atomic dimers of group II elements as well as organic molecular dimers. Second, the conformal vdW−QDO potential has better long-range

https://doi.org/10.1021/acs.jctc.3c00797
J. Chem. Theory Comput. 2023, 19, 7895−7907

behavior than the LJ and conformal TTS potentials. This is crucial for applications to extended systems where errors in the long-range vdW energy accumulate over many atomic pairs.

The key idea behind the presented potential is the synergy between vdW scaling laws, the coarse-grained QDO formalism for exchange repulsion, and the principle of corresponding states. In its current form, the vdW−QDO potential does not explicitly include the electrostatic contribution arising from charge penetration between atoms at short distances, which is non-negligible according to the SAPT. Although the short-range electrostatic interaction can be introduced into the QDO model in the form of a Coulomb integral,[55] this requires the introduction of an additional "electrostatic charge" parameter[36] into the vdW−QDO potential. Therefore, given the good accuracy of the current vdW−QDO potential, we decided to dispense with the explicit modeling of short-range electrostatics at this stage of model development. In its current version, the vdW−QDO potential can be incorporated into classical force fields as a nonempirical replacement for the LJ potential. For polar systems, an additional electrostatic/polarization term is needed in a force field (like it is done in the case of the LJ potential) to complete the description of noncovalent interactions.

We consider the present vdW−QDO potential as an important step toward a new generation of universal vdW potentials to be used in force fields and for biomolecular applications. To extract atom-in-molecule parameters, we currently employ *ab initio* calculations, which is a certain limitation. However, active development of machine-learning models[53,54,106] paves the way to obtain atom-in-molecule partitioning without costly electronic-structure calculations. Moreover, there is an increasing trend in creating extensive molecular data sets such as QM7-X,[107] which include information about atom-in-molecule volumes. This enables the direct applicability of the vdW−QDO potential to arbitrary molecular systems. Finally, the vdW−QDO potential can be generalized to include polarization and electrostatic contributions, which are the subject of our ongoing studies. Eventually, this effort should deliver a general coarse-grained force field for all noncovalent interactions entirely based on the model system of coupled QDOs.

■ ASSOCIATED CONTENT

Supporting Information

The Supporting Information is available free of charge at https://pubs.acs.org/doi/10.1021/acs.jctc.3c00797.

vdW-OQDO parameters for atomic dimers, derivation of the QDO damping function and the damped vdW−QDO potential, and results for eight molecular dimers (PDF)

■ AUTHOR INFORMATION

Corresponding Author

Alexandre Tkatchenko − *Department of Physics and Materials Science, University of Luxembourg, L-1511 Luxembourg City, Luxembourg;* orcid.org/0000-0002-1012-4854; Email: alexandre.tkatchenko@uni.lu

Authors

Almaz Khabibrakhmanov − *Department of Physics and Materials Science, University of Luxembourg, L-1511 Luxembourg City, Luxembourg;* orcid.org/0000-0003-3148-8064

Dmitry V. Fedorov − *Department of Physics and Materials Science, University of Luxembourg, L-1511 Luxembourg City, Luxembourg;* orcid.org/0000-0002-9949-5087

Complete contact information is available at: https://pubs.acs.org/10.1021/acs.jctc.3c00797

Notes

The authors declare no competing financial interest.

■ ACKNOWLEDGMENTS

We acknowledge financial support from the Luxembourg National Research Fund via FNR "ACTIVE (PRIDE19/14063202)" and "QuantPhonon (INTER/DFG/18/12944860)" projects as well as from the European Research Council (ERC Advanced Grant "FITMOL"). We thank Prof. Michał Tomza for providing us with the numerical data for the coupled-cluster potential curves of alkaline-earth dimers before their publication. We also thank Dr. Leonardo Medrano Sandonas (Uni.lu) for sharing his DFTB3+MBD results on molecular dimers.

■ REFERENCES

(1) Stone, A. *The Theory of Intermolecular Forces*; Oxford University Press, 2013.

(2) Kaplan, I. G. *Intermolecular Interactions: Physical Picture, Computational Methods and Model Potentials*; John Wiley & Sons, 2006.

(3) Israelachvili, J. N. *Intermolecular and Surface Forces*; Academic Press, 2011.

(4) Hermann, J.; DiStasio, R. A., Jr.; Tkatchenko, A. First-Principles Models for van der Waals Interactions in Molecules and Materials: Concepts, Theory, and Applications. *Chem. Rev.* **2017**, *117*, 4714−4758.

(5) Stöhr, M.; Van Voorhis, T.; Tkatchenko, A. Theory and practice of modeling van der Waals interactions in electronic-structure calculations. *Chem. Soc. Rev.* **2019**, *48*, 4118−4154.

(6) Case, D. A.; Cheatham, T. E., III; Darden, T.; Gohlke, H.; Luo, R.; Merz, K. M., Jr.; Onufriev, A.; Simmerling, C.; Wang, B.; Woods, R. J. The Amber biomolecular simulation programs. *J. Comput. Chem.* **2005**, *26*, 1668−1688.

(7) Brooks, B. R.; Brooks, C. L., III; Mackerell, A. D., Jr.; Nilsson, L.; Petrella, R. J.; Roux, B.; Won, Y.; Archontis, G.; Bartels, C.; Boresch, S.; et al. CHARMM: the biomolecular simulation program. *J. Comput. Chem.* **2009**, *30*, 1545−1614.

(8) Hess, B.; Kutzner, C.; Van Der Spoel, D.; Lindahl, E. GROMACS 4: algorithms for highly efficient, load-balanced, and scalable molecular simulation. *J. Chem. Theory Comput.* **2008**, *4*, 435−447.

(9) Jones, J. E. On the determination of molecular fields.—II. From the equation of state of a gas. *Proc. R. Soc. London, Ser. A* **1924**, *106*, 463−477.

(10) Buckingham, R. A. The classical equation of state of gaseous helium, neon and argon. *Proc. R. Soc. London, Ser. A* **1938**, *168*, 264−283.

(11) Barker, J.; Fisher, R.; Watts, R. Liquid argon: Monte Carlo and molecular dynamics calculations. *Mol. Phys.* **1971**, *21*, 657−673.

(12) Blaney, B. L.; Ewing, G. E. Van der Waals molecules. *Annu. Rev. Phys. Chem.* **1976**, *27*, 553−584.

(13) Tang, K. T.; Toennies, J. P. The van der Waals potentials between all the rare gas atoms from He to Rn. *J. Chem. Phys.* **2003**, *118*, 4976−4983.

(14) Tang, K.; Toennies, J. The dynamical polarisability and van der Waals dimer potential of mercury. *Mol. Phys.* **2008**, *106*, 1645−1653.

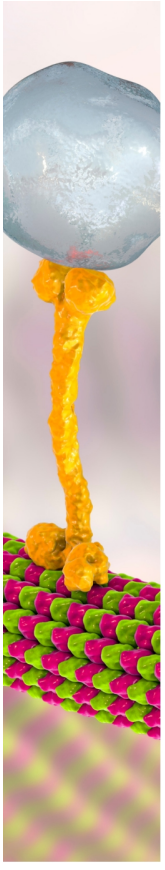
(15) Sheng, X.; Toennies, J. P.; Tang, K. Conformal Analytical Potential for All the Rare Gas Dimers over the Full Range of Internuclear Distances. *Phys. Rev. Lett.* **2020**, *125*, 253402.
(16) Sheng, X. W.; Tang, K. T. The development of a full range analytical interatomic potential. *Phys. Chem. Chem. Phys.* **2021**, *23*, 7748−7757.
(17) Jones, A. P.; Crain, J.; Sokhan, V. P.; Whitfield, T. W.; Martyna, G. J. Quantum Drude oscillator model of atoms and molecules: Many-body polarization and dispersion interactions for atomistic simulation. *Phys. Rev. B: Condens. Matter Mater. Phys.* **2013**, *87*, 144103.
(18) Heitler, W.; London, F. Wechselwirkung neutraler Atome und homöopolare Bindung nach der Quantenmechanik. *Z. Phys.* **1927**, *44*, 455−472.
(19) Slater, J. C. Molecular orbital and Heitler—London methods. *J. Chem. Phys.* **1965**, *43*, S11−S17.
(20) Fedorov, D. V.; Sadhukhan, M.; Stöhr, M.; Tkatchenko, A. Quantum-Mechanical Relation between Atomic Dipole Polarizability and the van der Waals Radius. *Phys. Rev. Lett.* **2018**, *121*, 183401.
(21) Vaccarelli, O.; Fedorov, D. V.; Stöhr, M.; Tkatchenko, A. Quantum-Mechanical Force Balance Between Multipolar Dispersion and Pauli Repulsion in Atomic van der Waals Dimers. *Phys. Rev. Res.* **2021**, *3*, 033181.
(22) Tkatchenko, A.; Fedorov, D. V.; Gori, M. Fine-Structure Constant Connects Electronic Polarizability and Geometric van-der-Waals Radius of Atoms. *J. Phys. Chem. Lett.* **2021**, *12*, 9488−9492.
(23) De Boer, J.; Michels, A. Contribution to the quantum-mechanical theory of the equation of state and the law of corresponding states. Determination of the law of force of helium. *Physica* **1938**, *5*, 945−957.
(24) De Boer, J. Quantum theory of condensed permanent gases I the law of corresponding states. *Physica* **1948**, *14*, 139−148.
(25) McQuarrie, D. A.; Simon, J. D. *Physical Chemistry: A Molecular Approach*; University Science Books, 1997; Vol. *1*.
(26) Rowlinson, J. S. *Cohesion: A Scientific History of Intermolecular Forces*; Cambridge University Press, 2002.
(27) Jeziorski, B.; Moszynski, R.; Szalewicz, K. Perturbation theory approach to intermolecular potential energy surfaces of van der Waals complexes. *Chem. Rev.* **1994**, *94*, 1887−1930.
(28) Szalewicz, K.; Jeziorski, B. Physical mechanisms of intermolecular interactions from symmetry-adapted perturbation theory. *J. Mol. Model.* **2022**, *28*, 273.
(29) Tkatchenko, A.; Scheffler, M. Accurate Molecular Van Der Waals Interactions from Ground-State Electron Density and Free-Atom Reference Data. *Phys. Rev. Lett.* **2009**, *102*, 073005.
(30) Řezáč, J.; Riley, K. E.; Hobza, P. S66: A well-balanced database of benchmark interaction energies relevant to biomolecular structures. *J. Chem. Theory Comput.* **2011**, *7*, 2427−2438.
(31) Bade, W. L. Drude-model calculation of dispersion forces. I. General theory. *J. Chem. Phys.* **1957**, *27*, 1280−1284.
(32) Thole, B. Molecular polarizabilities calculated with a modified dipole interaction. *Chem. Phys.* **1981**, *59*, 341−350.
(33) Wang, F.; Jordan, K. D. A Drude-model approach to dispersion interactions in dipole-bound anions. *J. Chem. Phys.* **2001**, *114*, 10717−10724.
(34) Sommerfeld, T.; Jordan, K. D. Quantum Drude Oscillator Model for Describing the Interaction of Excess Electrons with Water Clusters: An Application to $(H_2O)_{13}^-$. *J. Phys. Chem. A* **2005**, *109*, 11531−11538.
(35) Jones, A. *Quantum Drude Oscillators for Accurate Many-Body Intermolecular Forces*. Ph.D. Thesis, The University of Edinburgh, 2010.
(36) Cipcigan, F. S.; Crain, J.; Sokhan, V. P.; Martyna, G. J. Electronic coarse graining: Predictive atomistic modeling of condensed matter. *Rev. Mod. Phys.* **2019**, *91*, 025003.
(37) Whitfield, T. W.; Martyna, G. J. A unified formalism for many-body polarization and dispersion: The quantum Drude model applied to fluid xenon. *Chem. Phys. Lett.* **2006**, *424*, 409−413.
(38) Jones, A.; Cipcigan, F.; Sokhan, V. P.; Crain, J.; Martyna, G. J. Electronically Coarse-Grained Model for Water. *Phys. Rev. Lett.* **2013**, *110*, 227801.
(39) Sokhan, V. P.; Jones, A. P.; Cipcigan, F. S.; Crain, J.; Martyna, G. J. Signature properties of water: Their molecular electronic origins. *Proc. Natl. Acad. Sci. U.S.A.* **2015**, *112*, 6341−6346.
(40) Tkatchenko, A.; DiStasio, R. A., Jr.; Car, R.; Scheffler, M. Accurate and Efficient Method for Many-Body van der Waals Interactions. *Phys. Rev. Lett.* **2012**, *108*, 236402.
(41) Ambrosetti, A.; Alfè, D.; DiStasio, R. A., Jr.; Tkatchenko, A. Hard numbers for large molecules: Toward exact energetics for supramolecular systems. *J. Phys. Chem. Lett.* **2014**, *5*, 849−855.
(42) Ambrosetti, A.; Umari, P.; Silvestrelli, P. L.; Elliott, J.; Tkatchenko, A. Optical van-der-Waals forces in molecules: from electronic Bethe-Salpeter calculations to the many-body dispersion model. *Nat. Commun.* **2022**, *13*, 813.
(43) Karimpour, M. R.; Fedorov, D. V.; Tkatchenko, A. Quantum framework for describing retarded and nonretarded molecular interactions in external electric fields. *Phys. Rev. Res.* **2022**, *4*, 013011.
(44) Karimpour, M. R.; Fedorov, D. V.; Tkatchenko, A. Molecular Interactions Induced by a Static Electric Field in Quantum Mechanics and Quantum Electrodynamics. *J. Phys. Chem. Lett.* **2022**, *13*, 2197−2204.
(45) Góger, S.; Khabibrakhmanov, A.; Vaccarelli, O.; Fedorov, D. V.; Tkatchenko, A. Optimized Quantum Drude Oscillators for Atomic and Molecular Response Properties. *J. Phys. Chem. Lett.* **2023**, *14*, 6217−6223.
(46) Ambrosetti, A.; Silvestrelli, P. L. van der Waals interactions in density functional theory using Wannier functions: Improved C_6 and C_3 coefficients by a different approach. *Phys. Rev. B: Condens. Matter Mater. Phys.* **2012**, *85*, 073101.
(47) Johnson, E. R. *Non-covalent Interactions in Quantum Chemistry and Physics*; Otero-de-la-Roza, A., DiLabio, G. A., Eds.; Elsevier, 2017; Chapter 5, pp 169−194.
(48) Grimme, S.; Hansen, A.; Brandenburg, J. G.; Bannwarth, C. Dispersion-Corrected Mean-Field Electronic Structure Methods. *Chem. Rev.* **2016**, *116* (9), 5105−5154.
(49) Harder, E.; Anisimov, V. M.; Vorobyov, I. V.; Lopes, P. E. M.; Noskov, S. Y.; MacKerell, A. D.; Roux, B. Atomic Level Anisotropy in the Electrostatic Modeling of Lone Pairs for a Polarizable Force Field Based on the Classical Drude Oscillator. *J. Chem. Theory Comput.* **2006**, *2*, 1587−1597.
(50) Lopes, P. E. M.; Huang, J.; Shim, J.; Luo, Y.; Li, H.; Roux, B.; MacKerell, A. D. Polarizable Force Field for Peptides and Proteins Based on the Classical Drude Oscillator. *J. Chem. Theory Comput.* **2013**, *9*, 5430−5449.
(51) Adluri, A. N. S.; Murphy, J. N.; Tozer, T.; Rowley, C. N. Polarizable Force Field with a σ-Hole for Liquid and Aqueous Bromomethane. *J. Phys. Chem. B* **2015**, *119*, 13422−13432.
(52) Poier, P. P.; Lagardère, L.; Piquemal, J.-P. O(N) Stochastic Evaluation of Many-Body van der Waals Energies in Large Complex Systems. *J. Chem. Theory Comput.* **2022**, *18*, 1633−1645.
(53) Muhli, H.; Chen, X.; Bartók, A. P.; Hernández-León, P.; Csányi, G.; Ala-Nissila, T.; Caro, M. A. Machine learning force fields based on local parametrization of dispersion interactions: Application to the phase diagram of C 60. *Phys. Rev. B* **2021**, *104*, 054106.
(54) Poier, P. P.; Jaffrelot Inizan, T.; Adjoua, O.; Lagardere, L.; Piquemal, J.-P. Accurate Deep Learning-Aided Density-Free Strategy for Many-Body Dispersion-Corrected Density Functional Theory. *J. Phys. Chem. Lett.* **2022**, *13*, 4381−4388.
(55) Sadhukhan, M.; Manby, F. R. Quantum mechanics of Drude oscillators with full Coulomb interaction. *Phys. Rev. B* **2016**, *94*, 115106.
(56) Born, M.; Mayer, J. E. Zur gittertheorie der ionenkristalle. *Z. Phys.* **1932**, *75*, 1−18.
(57) Hellmann, R.; Bich, E.; Vogel, E. Ab initio potential energy curve for the neon atom pair and thermophysical properties of the dilute neon gas. I. Neon−neon interatomic potential and rovibrational spectra. *Mol. Phys.* **2008**, *106*, 133−140.

https://doi.org/10.1021/acs.jctc.3c00797
J. Chem. Theory Comput. 2023, 19, 7895−7907

(58) Duman, E. L.; Smirnov, B. M. Exchange interaction of multi-electron atoms. *Opt. Spectrosc.* **1970**, *29*, 229−233.
(59) Kleinekathöfer, U.; Tang, K.; Toennies, J.; Yiu, C. Angular momentum coupling in the exchange energy of multielectron systems. *J. Chem. Phys.* **1995**, *103*, 6617−6630.
(60) Tang, K. T.; Toennies, J. P.; Yiu, C. L. The generalized Heitler-London theory for interatomic interaction and surface integral method for exchange energy. *Int. Rev. Phys. Chem.* **1998**, *17*, 363−406.
(61) Salem, L. The forces between polyatomic molecules. II. Short-range repulsive forces. *Proc. R. Soc. London, Ser. A* **1961**, *264*, 379−391.
(62) Rackers, J. A.; Ponder, J. W. Classical Pauli repulsion: An anisotropic, atomic multipole model. *J. Chem. Phys.* **2019**, *150*, 084104.
(63) Tang, K.; Toennies, J. P. New combining rules for well parameters and shapes of the van der Waals potential of mixed rare gas systems. *Z. Phys. D* **1986**, *1*, 91−101.
(64) Van Vleet, M. J.; Misquitta, A. J.; Stone, A. J.; Schmidt, J. R. Beyond Born−Mayer: Improved models for short-range repulsion in ab initio force fields. *J. Chem. Theory Comput.* **2016**, *12*, 3851−3870.
(65) Bondi, A. van der Waals volumes and radii. *J. Phys. Chem.* **1964**, *68*, 441−451.
(66) Gobre, V. V. *Efficient Modelling of Linear Electronic Polarization in Materials Using Atomic Response Functions*. Ph.D. Thesis, Fritz Haber Institute Berlin, 2016.
(67) Jiang, J.; Mitroy, J.; Cheng, Y.; Bromley, M. Effective oscillator strength distributions of spherically symmetric atoms for calculating polarizabilities and long-range atom−atom interactions. *At. Data Nucl. Data* **2015**, *101*, 158−186.
(68) Farrar, J. M.; Schafer, T.; Lee, Y.-T. Intermolecular potentials of symmetric rare gas pairs from elastic differential cross section measurements. *AIP Conf. Proc.* **1973**, *11*, 279−295.
(69) Tang, K. T.; Toennies, J. P. A simple theoretical model for the van der Waals potential at intermediate distances. I. Spherically symmetric potentials. *J. Chem. Phys.* **1977**, *66*, 1496−1506.
(70) Cencek, W.; Przybytek, M.; Komasa, J.; Mehl, J. B.; Jeziorski, B.; Szalewicz, K. Effects of adiabatic, relativistic, and quantum electrodynamics interactions on the pair potential and thermophysical properties of helium. *J. Chem. Phys.* **2012**, *136*, 224303.
(71) Patkowski, K.; Szalewicz, K. Argon pair potential at basis set and excitation limits. *J. Chem. Phys.* **2010**, *133*, 094304.
(72) Jäger, B.; Hellmann, R.; Bich, E.; Vogel, E. State-of-the-art ab initio potential energy curve for the krypton atom pair and thermophysical properties of dilute krypton gas. *J. Chem. Phys.* **2016**, *144*, 114304.
(73) Hellmann, R.; Jäger, B.; Bich, E. State-of-the-art ab initio potential energy curve for the xenon atom pair and related spectroscopic and thermophysical properties. *J. Chem. Phys.* **2017**, *147*, 034304.
(74) López Cacheiro, J.; Fernández, B.; Marchesan, D.; Coriani, S.; Hättig, C.; Rizzo, A. Coupled cluster calculations of the ground state potential and interaction induced electric properties of the mixed dimers of helium, neon and argon. *Mol. Phys.* **2004**, *102*, 101−110.
(75) Haley, T. P.; Cybulski, S. M. Ground state potential energy curves for He−Kr, Ne−Kr, Ar−Kr, and Kr 2: Coupled-cluster calculations and comparison with experiment. *J. Chem. Phys.* **2003**, *119*, 5487−5496.
(76) Shee, A.; Knecht, S.; Saue, T. A theoretical benchmark study of the spectroscopic constants of the very heavy rare gas dimers. *Phys. Chem. Chem. Phys.* **2015**, *17*, 10978−10986.
(77) Delhommelle, J.; Millié, P. Inadequacy of the Lorentz-Berthelot combining rules for accurate predictions of equilibrium properties by molecular simulation. *Mol. Phys.* **2001**, *99*, 619−625.
(78) Song, W.; Rossky, P. J.; Maroncelli, M. Modeling alkane+ perfluoroalkane interactions using all-atom potentials: failure of the usual combining rules. *J. Chem. Phys.* **2003**, *119*, 9145−9162.
(79) Boda, D.; Henderson, D. The effects of deviations from Lorentz−Berthelot rules on the properties of a simple mixture. *Mol. Phys.* **2008**, *106*, 2367−2370.
(80) Tang, K. Dynamic polarizabilities and van der Waals coefficients. *Phys. Rev.* **1969**, *177*, 108−114.
(81) Lejaeghere, K.; Van Speybroeck, V.; Van Oost, G.; Cottenier, S. Error estimates for solid-state density-functional theory predictions: an overview by means of the ground-state elemental crystals. *Crit. Rev. Solid State Mater. Sci.* **2014**, *39*, 1−24.
(82) Lejaeghere, K.; Bihlmayer, G.; Björkman, T.; Blaha, P.; Blügel, S.; Blum, V.; Caliste, D.; Castelli, I. E.; Clark, S. J.; Dal Corso, A.; et al. Reproducibility in density functional theory calculations of solids. *Science* **2016**, *351*, aad3000.
(83) Tang, K. T.; Toennies, J. P. An improved simple model for the van der Waals potential based on universal damping functions for the dispersion coefficients. *J. Chem. Phys.* **1984**, *80*, 3726−3741.
(84) Yang, D.; Li, P.; Tang, K. The ground state van der Waals potentials of the calcium dimer and calcium rare-gas complexes. *J. Chem. Phys.* **2009**, *131*, 154301.
(85) Li, P.; Xie, W.; Tang, K. The van der Waals potential of the magnesium dimer. *J. Chem. Phys.* **2010**, *133*, 084308.
(86) Yin, G.; Li, P.; Tang, K. The ground state van der Waals potentials of the strontium dimer and strontium rare-gas complexes. *J. Chem. Phys.* **2010**, *132*, 074303.
(87) Li, P.; Ren, J.; Niu, N.; Tang, K. Corresponding states principle for the alkaline earth dimers and the van der waals potential of Ba2. *J. Phys. Chem. A* **2011**, *115*, 6927−6935.
(88) Wei, L.; Li, P.; Qiao, L.; Tang, K. Corresponding states principle and van der Waals potentials of Zn2, Cd2, and Hg2. *J. Chem. Phys.* **2013**, *139*, 154306.
(89) Wei, L.; Li, P.; Tang, K. The van der Waals potentials of MgCa, MgSr, MgBa, CaSr, CaBa, and SrBa. *Chem. Phys. Lett.* **2015**, *635*, 285−289.
(90) Porsev, S. G.; Derevianko, A. High-accuracy calculations of dipole, quadrupole, and octupole electric dynamic polarizabilities and van der Waals coefficients C6, C8, and C10 for alkaline-earth dimers. *J. Exp. Theor. Phys.* **2006**, *102*, 195−205.
(91) Ladjimi, H.; Tomza, M. Diatomic molecules of alkali-metal and alkaline-earth-metal atoms: interaction potentials, dipole moments, and polarizabilities. **2023**, arXiv:2303.17527.
(92) Schwerdtfeger, P.; Nagle, J. K. 2018 Table of static dipole polarizabilities of the neutral elements in the periodic table. *Mol. Phys.* **2019**, *117*, 1200−1225.
(93) Zaremba-Kopczyk, K.; Tomza, M. Van der Waals molecules consisting of a zinc or cadmium atom interacting with an alkali-metal or alkaline-earth-metal atom. *Phys. Rev. A* **2021**, *104*, 042816.
(94) Pahl, E.; Figgen, D.; Thierfelder, C.; Peterson, K. A.; Calvo, F.; Schwerdtfeger, P. A highly accurate potential energy curve for the mercury dimer. *J. Chem. Phys.* **2010**, *132*, 114301.
(95) Tiesinga, E.; Kotochigova, S.; Julienne, P. S. Scattering length of the ground-state Mg+ Mg collision. *Phys. Rev. A* **2002**, *65*, 042722.
(96) Allard, O.; Pashov, A.; Knöckel, H.; Tiemann, E. Ground-state potential of the Ca dimer from Fourier-transform spectroscopy. *Phys. Rev. A* **2002**, *66*, 042503.
(97) Stein, A.; Knöckel, H.; Tiemann, E. Fourier-transform spectroscopy of Sr 2 and revised ground-state potential. *Phys. Rev. A* **2008**, *78*, 042508.
(98) Adamo, C.; Barone, V. Toward reliable density functional methods without adjustable parameters: The PBE0 model. *J. Chem. Phys.* **1999**, *110*, 6158−6170.
(99) Perdew, J. P.; Ernzerhof, M.; Burke, K. Rationale for mixing exact exchange with density functional approximations. *J. Chem. Phys.* **1996**, *105* (22), 9982−9985.
(100) Hourahine, B.; Aradi, B.; Blum, V.; Bonafé, F.; Buccheri, A.; Camacho, C.; Cevallos, C.; Deshaye, M. Y.; Dumitrică, T.; Dominguez, A.; et al. DFTB+, a software package for efficient approximate density functional theory based atomistic simulations. *J. Chem. Phys.* **2020**, *152*, 124101.
(101) Blum, V.; Gehrke, R.; Hanke, F.; Havu, P.; Havu, V.; Ren, X.; Reuter, K.; Scheffler, M. Ab initio molecular simulations with numeric atom-centered orbitals. *Comput. Phys. Commun.* **2009**, *180*, 2175−2196.

https://doi.org/10.1021/acs.jctc.3c00797
J. Chem. Theory Comput. 2023, 19, 7895−7907

(102) Heßelmann, A. DFT-SAPT intermolecular interaction energies employing exact-exchange Kohn−Sham response methods. *J. Chem. Theory Comput.* **2018**, *14*, 1943−1959.
(103) Hermann, J.; Alfè, D.; Tkatchenko, A. Nanoscale $\pi-\pi$ stacked molecules are bound by collective charge fluctuations. *Nat. Commun.* **2017**, *8*, 14052.
(104) Stöhr, M.; Medrano Sandonas, L.; Tkatchenko, A. Accurate many-body repulsive potentials for density-functional tight binding from deep tensor neural networks. *J. Phys. Chem. Lett.* **2020**, *11*, 6835−6843.
(105) Podeszwa, R.; Pernal, K.; Patkowski, K.; Szalewicz, K. Extension of the Hartree- Fock plus dispersion method by first-order correlation effects. *J. Phys. Chem. Lett.* **2010**, *1*, 550−555.
(106) Westermayr, J.; Chaudhuri, S.; Jeindl, A.; Hofmann, O. T.; Maurer, R. J. Long-range dispersion-inclusive machine learning potentials for structure search and optimization of hybrid organic−inorganic interfaces. *Digital Discovery* **2022**, *1*, 463−475.
(107) Hoja, J.; Medrano Sandonas, L.; Ernst, B. G.; Vazquez-Mayagoitia, A.; DiStasio, R. A., Jr.; Tkatchenko, A. QM7-X, a comprehensive dataset of quantum-mechanical properties spanning the chemical space of small organic molecules. *Sci. Data* **2021**, *8*, 43.


CAS BIOFINDER DISCOVERY PLATFORM™
BRIDGE BIOLOGY AND CHEMISTRY FOR FASTER ANSWERS
Analyze target relationships, compound effects, and disease pathways
Explore the platform
CAS
A division of the American Chemical Society

https://doi.org/10.1021/acs.jctc.3c00797
J. Chem. Theory Comput. 2023, 19, 7895−7907